Technical Notes
August 2022
Issue TN0291

OPA - Ocean Predictions and Applications Division

Climate Projections of salt-wedge intrusions in a Po river branch (Northern Adriatic Sea)

By ***Sahameddin M. Kurdistani***
Fondazione CMCC Centro Euro-Mediterraneo sui Cambiamenti Climatici Lecce, Italy

Giorgia Verri*
Fondazione CMCC Centro Euro-Mediterraneo sui Cambiamenti Climatici Lecce, Italy giorgia.verri@cmcc.it

Nadia Pinardi
Alma Mater Studiorum Università di Bologna, Department of Physics and Astronomy, Bologna, Italy

Giovanni Coppini
Fondazione CMCC Centro Euro-Mediterraneo sui Cambiamenti Climatici Lecce, Italy

SUMMARY Estuaries are the transitional systems between the riverine freshwaters and the ocean salt water. Increasing salt-wedge intrusions are mentioned as one of the major impacts of climate change in coastal areas. We propose a new methodology to predict salt wedge intrusions with an intermediate complexity model, so-called Estuarine Box Model (EBM), that allows to use hydrology and ocean climate scenarios to predict salt wedge intrusions. We apply this methodology to the Goro branch of the Po river flowing into the Northern Adriatic Sea for both present and future climate conditions. A 30 years period (1982-2011) is used to train and test the EBM that is then used to project the salt wedge in the (2021-2050) time period under the RCP8.5 emission scenario. The numerical results show that in the (2021-2050) period, the Po di Goro salt wedge intrusion length will increase by 15% on an annual basis (up to 50% in summertime) and the outflowing salinity will increase 9% on annual basis (up to 35% in summer). Finally, a statistical estimation of the extreme values of salt wedge and outflowing salinity shows return periods of 10 years for extremes twice the present mean values. It means that a 16 Km of salt-wedge intrusion, and outgoing salinity about 28 psu are highly expected as an extreme event with 10 years return period.

Keywords Climate projections, salt-wedge intrusion, river estuary

**Correspondence to*: Giorgia Verri (giorgia.verri@cmcc.it)

1. INTRODUCTION

River salt-wedge intrusions are important threats to the quality of inland waters (Green, 2016). Regionally downscaled climate change scenarios do not properly consider the river salt-wedge intrusions because their grid spacing cannot represent the estuary geometry and they do not involve a proper river-seawater coupling. If we want to gain insight on the trends of salt wedge intrusions along the river estuaries, even with present day IPCC climate scenario model results, we need to couple regional climate models with intermediate complexity models that can link the changes in river runoff with the coastal sea and represent the estuarine mixing processes.

Recent literature on salt-wedge intrusion (SWI) projections has considered the changes in the upstream river flow and the sea level rise (SLR) under different climate change scenarios (Yeung Leung et al., 2018; Bellafiore et al., 2021). The overall result is that the river discharge changes are expected to affect the SWI more than the SLR. A source of uncertainty is represented by the use of global or at most regional scale SLR (Adloff et al, 2018) without considering the local effects probably because no regional downscaled scenario reaches the resolution required to resolve the local SLR (Somot et al., 2018; Torresan et al., 2019). An additional challenge is the computational resources required to perform long term numerical experiments with very high-resolution hydrology and ocean models to resolve the estuary geometry. For this reason, the SWI response to climate change has been evaluated by means of synthetic experiments and/or annual mean experiments with upstream river runoff and ocean water inflow averaged over multi-decadal time windows representing the present and future climate. There is a need to have an intermediate complexity model (Claussen et al., 2002) that is capable to run many decades, with inputs from the hydrological changes upstream the estuary and the ocean saltwater changes at the estuary mouth.

In the past 10 years, other studies have simulated the temporal variability of the SWI length. MacCready and Geyer (2010) provided an empirical estimate of this length scale in river-dominated estuaries and the EBM presented in Sun et al. (2018) followed this formulation. The current study uses a novel, intermediate complexity model, the so-called CMCC EBM model (Verri et al., 2020; Verri et al., 2021), which solves the estuarine water exchange by two conservation equations for volume and salt averaged over the diurnal tidal cycle and uses a parametric equation for the SWI length (Appendix A). The EBM has been applied to the Goro branch of the Po river which is a river-dominated estuary and flows into the micro-tidal Adriatic Sea (Fig. 1).

The main aim of this study is to show how to predict SWI and outflowing estuarine-water salinity with an intermediate complexity model, encompassing the main estuarine dynamics processes.

The question asked is: is the salt-wedge changing in the future climate scenarios and why? To what degree the estuarine dynamics is dominated by changes in the upstream river discharge?

In section 2 we describe the modelling strategy and the forcing data used to perform the climate experiments. Section 3 presents the results on the salt-wedge intrusion scenario and the changes in outflowing salinity. Moreover, a statistical estimation of the extreme values is provided. Conclusions are offered in section 4.

2. METHODOLOGY

2.1 MODELLING STRATEGY

The use of intermediate complexity models in climate coastal impact studies is important because the earth system climate models do not have enough resolution to account for the complex coastal geometry and local processes. This is the case of estuarine areas where the freshwater meets the saltwater and eventually give rise to

SWI phenomena and river plumes on the offshore area of the estuary that might affect primary, secondary and tertiary marine production (Watanabe et al., 2014; James et al., 2013) in addition to groundwater salt contamination. The more recent earth system models are still not able to properly couple model components at the land-sea interface (Claussen et al., 2002; Adloff et al, 2018; Somot et al., 2018; Torresan et al., 2019) and in order to study the interactions between river waters and the sea it is necessary to use intermediate complexity models such as the Estuarine Box Model of this study.

The two unknowns of our study are the SWI length and the salinity of the outflowing waters: the first has obvious implications for the above-mentioned salinization of inland waters and the second affects the coastal circulation and dynamics off the river mouths, i.e. the river plume, as well as the large-scale circulation (Verri et al., 2018, Guangpeng et al., 2022).

2.2 RIVER FORCING: HISTORICAL DATA AND CLIMATE PROJECTIONS

For the historical (1982 – 2011) period, the Po river discharge was taken from observations at Pontelagoscuro hydrometer station (Fig.1), a location upstream of the Po delta river branches. The scenario of the Po discharge has been predicted by Vezzoli et al. (2015) using a hydrological model forced by a regional atmospheric model (Bucchignani et al., 2014) nested in a global earth system climate model (Scoccimarro et al., 2011). Vezzoli et al. (2015) computed the RCP8.5 scenario projections for the Po at Pontelagoscuro. Figure 2a depicts daily discharge values observed during the (1982 – 2011) period having a time mean discharge of 1482 m^3/s while Fig. 2b shows the predicted discharge for Po at Pontelagoscuro for the scenario period (2021–2050) amounting to 1205 m^3/s. Thus, the mean annual discharge of the Po river is reduced in the future period by approximately 23% with respect to the present conditions. We estimate the Goro branch of the Po river receives about 13% of the discharge at Pontelagoscuro (Verri et al., 2021) so in all our calculations we will use the upstream Po di Goro discharge value as the Po discharge at Pontelagoscuro scaled by 0.13.

2.3 OCEAN FORCING: HISTORICAL DATA AND CLIMATE PROJECTIONS

The EBM considers a two-layer flow in the estuary averaged over the estuarine horizontal areas and the equations are described in Appendix A. The lower layer inflowing salinity, S_{ll}, and volume flux, Q_{ll}, for both the past state and the future scenario period were taken from the ocean component of a regional climate model (Cavicchia et al., 2015). The Q_{ll} shows an average value of 3.3 m^3/s in the historical period while 3.1 m^3/s for the scenario period, corresponding to a decrease of about 6%. The S_{ll} values show mean values of 35.3 psu for the historical period and 35.6 psu for the scenario period indicating a 1% increase.

The volume flux due to the flood tides Q_{tidef} is taken from the OTPS astronomical tidal model in its regional configuration over the Mediterranean Sea with 1/30-degree horizontal resolution (Egbert and Erofeeva, 2002). The mean tidal flow, extracted during the diurnal flood tide phases and averaged over 30 years, amounts to 18.6 m^3/s for the historical period and 18.7 m^3/s for the scenario period, given the short period considered for astronomical parameters to change. Thus, all the ocean lateral boundary conditions change relatively little with respect to the river discharge and this strongly affect the salt-wedge projections.

3. RESULTS

3.1 SALT-WEDGE INTRUSION PROJECTIONS

Using the CMCC-EBM model, the SWI length L_x and the outflowing upper layer salinity S_{ul} have been computed for both historical and scenario periods. Figure 3 shows the values of L_x for the historical period (1982-2011) with the long-term average value of L_x = 8.1 Km. For the scenario period (2021– 2050) L_x increases by 1.2 km, i.e. a 15% increase over the present condition values.

Similarly, the outflowing upper layer salinity is higher as shown in Figure 4(a, b) where the salinity at the river mouth will increase of 1.1 psu in the mid-term scenario with respect to the present climate (corresponding to a 9% increase on annual basis).

The comparison of the seasonal daily mean values over the two 30 years' periods for L_x and S_{ul} is shown in Fig. 5(a, b). The (2021-2050) projections show a larger increase of L_x during summer, arriving to a 40% increase in the July-August period with respect to present conditions. For the outflowing upper layer salinity, we see an increase from 20 to 25 psu during the summer months. In the (2020-2050) period we expect the salinity at river mouth will rise up to 35% in summer while a decrease is foreseen over November-January.

In conclusions we argue that the river discharge is the driver of SWI length and the salinity changes at the river mouth, neglecting the local SLR trends at the river mouth that now are not known. The mean SLR over the Adriatic Sea is about 3 mm/year (Bonaduce et al., 2016) from satellite altimetry and tide gauges. If we suppose this growth to be true in the future climate period, 2021-2050, and that this growth is solely balanced by a net transport at the Otranto Strait we obtain a transport of ~130 m3/sec (Appendix C) that is, with respect to the present value of transport, 0.1 % of the measured net transport equal to 10000 m3/sec (Yari et al., 2012). Supposedly the change at the river mouth could be of that order of magnitude and thus we considered it negligible.

The other forcing changes, such as the inflowing lower layer salinity and volume flux are negligible with respect to upstream discharge changes. Nevertheless, even knowing the changes upstream and downstream of the river, it will be impossible to calculate the exact changes in SWI length without the CMCC-EBM which encompasses all the necessary physical processes.

3.2 EXTREME VALUES ESTIMATION

In addition to the projection of SWI changes with respect to the present climate, it is important to define the probability of extreme events in terms of return periods. The Peak Over Threshold (POT) (Leadbetter, 1991) method has been used to generate the input dataset of the extreme values of SWI lengths and outflowing upper layer salinity. One of the key choices in the POT method is to decide a threshold value. For the extreme values, the threshold has been considered as the minimum value of the yearly maximum values during the historical period (1982-2011) which produces the threshold values of 12 Km for L_x and 23 psu for S_{ul}.

Literature shows that the Probability Density Function (PDF) of positive definite atmospheric and ocean variables are skewed and heavy-tailed (Sepp Neves et al., 2020; Sardeshmukh and Compo, 2015). Figure 6(a, b) shows that the frequencies of occurrence of the daily values of L_x and S_{ul} follow a Weibull PDF (Weibull, 1951) for both parameters. The Bootstrap percentile method (Efron, 1979; Efron and Tibshirani, 1994; Meeker et al., 2017) has been applied to compute the confidence intervals of the parameters β and σ as the "shape" and "scale" parameters of the Weibull PDF for the data of L_x and S_{ul}. Details are given in Appendix B.

The probability curves of the extreme values of the L_x and S_{ul} as function of their return periods T along with the upper and lower 95% confidence intervals are shown in Fig. 7a and Fig. 7b respectively. The return period is by definition $T = \frac{1}{1-P_{x \le x_{max}}}$ where $P_{x \le x_{max}}$ is the Weibull cumulative distribution function representing the probability that the variable x (L_x and S_{ul} in this work) is less than or equal to the selected threshold x_{max}.

The SWI extreme values of 16 km and 20 km registered during the historical period (when the mean SWI length is found to be equal to 8.1 km) are expected with 10 and 100 years return periods respectively. Red points in Fig. 7a are the projected values of

L_x by the EBM model for the scenario period (2021-2050). In the projections L_x values of 20 km will have a shorter return period of about 60 years.

Moreover, the river mouth salinity extreme values of 28 psu and 34 psu registered during the historical period (when the mean outflowing salinity at river mouth is found to be equal to 12.9 psu) are also expected to occur with 10 and 100 years return periods (Fig. 7b). Red points in Fig. 7b are the projected values of S_{ul} by EBM model for the scenario period (2021-2050) and the 34 psu values will have a shorter return period of about 50 years.

Overall the SWI and S_{ul} extreme values have shorter short return periods in the future climate: return periods of 10 years (high occurrence probability) are found for extremes corresponding to twice the present mean values.

4. CONCLUSIONS

An intermediate complexity estuarine box model, so-called CMCC-EBM, has been used for the first time as an intermediate complexity model to study SWI and outflowing salinity in rivers for present and future climate conditions. The CMCC-EBM couples the hydrology and the shelf ocean waters from general circulation models.

This study shows that, for a river-dominated estuary flowing into a micro-tidal sea, the river discharge reduction is the main factor affecting the increase of the SWI and the river outflowing salinity. Assuming a constant sea level rise trend, the volume flux associated with the sea level rise is small as well as the changes in tides for the period 2021-2050. The numerical findings for the Po di Goro river branch depict an average lengthening of the SWI in the (2021-2050) period equal to 1.2 km (meaning a 15% increase) and an increase of the river outflowing salinity of 1.1 psu (corresponding to a 9% increase). This increase has a large seasonal cycle, the projections showing a sharp increase in summer time for the SWI length and the salinity up to 40-50% of the present state values.

The extreme values of SWI and outflowing salinity computed for the climate projections have shorter return periods. SWI maximum values such as 20 km, have return periods of 100 years for the historical period and about 60 years in the projected climate.

Overall the projected changes in the SWI length of the Po di Goro branch provide a valuable piece of information for adaptation policies since it is already clear that this region is facing increasing salinization of inland waters. Furthermore, it is known that a change of several psu in river outflowing salinity has the potential of changing the ocean circulation and dynamics from coastal to large scales (Verri et al., 2018). For all these reasons above, the CMCC-EBM intermediate complexity model used here could be a valuable hazard informing tool for coastal adaptation plans.

APPENDIX A: THE ESTUARINE BOX MODEL

The CMCC EBM (Verri et al., 2020; Verri et al., 2021), (http://www.estuaryboxmodel.org) assumes a two-layer flow dynamics in the estuary. The continuity equation and the salinity advection-diffusion equation are integrated in each layer and across the horizontal dimensions of the estuary, its length and width (see Fig. A1). This produces conservation equations for the volume flux and the salt flux supposed to be uniform in each layer. The two resulting equations are:

$$Q_{ul} = Q_{river} + Q_{ll} + H\,L_y u_{tidef} \quad (1)$$

$$S_{ul} = S_{ul}Q_{ul} + \bar{S}\,HL_y u_{tidef} + K_{SH}HL_y \frac{\bar{S}}{L_x} \quad (2)$$

where H, L_y, L_x the estuary depth, width and length respectively. Here we assume L_y= 200 m and H=5 m as in Verri et al. (2021). The subscripts "*ul*" and "*ll*" refer to the upper and lower estuary layers respectively, u_{tidef} is the barotropic velocity corresponding to the flood tide phase, $\bar{S}$ is the depth averaged ocean salinity and K_{SH} = C_k L_y u_{tidef}, the horizontal eddy diffusivity where C_k is the non-dimensional eddy diffusivity coefficient representative of the estuary stratification. Verri et al. (2021) by means of a dimensional analysis conducted based on the theorem of Buckingham and Self-Similarity (Barenblatt, 1987; Kurdistani et al., 2019) presented a parametric equation to determine C_k. The lateral ocean input fields at the estuary mouth are: Q_{ll}, S_{ll}, $\bar{S}$ and u_{tidef}. The river volume flux Q_{river} has to be provided at the estuary head, i.e. at the last section along the river network moving in the downstream direction where the salinity is still equal to zero on multi-year average conditions.

The estuary length in CMCC-EBM is considered to represent the Salt-Wedge Intrusion (SWI) length which changes dynamically following a parametric equation developed by Verri et al. (2021) for the Goro branch of the Po river:

$$L_x = 10\,H\,F_r^{-0.3}\left(\frac{\rho_{ll}}{\rho_0}\right)^{40}\left(\frac{H}{h}\right)^{-4.6}\left(\frac{Q_{tidef}}{Q_{river}}\right)^{0.3}\left(\frac{Q_{ll}}{Q_{river}}\right)^{-0.01} \quad (3)$$

where F_r is the river Froude number, $Q_{tidef} = L_y\,H\,u_{tidef}$, ρ_0=1000 kgm^{-3} is the river freshwater density, $\rho_{ll} = \rho_0\,(1+k_s\,S_{ll})$ with the haline contraction coefficient taken to be constant and equal to $k_s = 7.7 \times 10^{-4}$ psu^{-1} (Verri et al., 2021).

These three equations will give estimates of the outflowing volume flux Q_{ul}, the salinity S_{ul} and the SWI length L_x which we propose as an impact model to be interfaced with the climate projected input fields for Q_{river} and Q_{ll}, S_{ll}, $\bar{S}$ and u_{tidef}.

APPENDIX B: THE CONFIDENCE LEVELS OF THE EXTREME VALUES

As it has been explained in the main body of the paper, the Peak Over Threshold (POT) method has been employed to define the probability of extreme events observed during the historical range in terms of their return periods. The POT datasets of the extreme values of SWI lengths and outflowing salinity are the historical daily values which exceed a threshold defined as the minimum value of the yearly maximum values, i.e. 12km and 23psu respectively.

Figure 6(a, b) shows that the frequencies of occurrence of the POT daily values of both L_x and S_{ul} follow a Weibull probability density function PDF (Efron and Tibshirani, 1994).

The Bootstrap percentile method (Meeker et al., 2017) has been applied to compute the confidence intervals of the "shape" and "scale" parameters of the Weibull distribution for extreme L_x and S_{ul} shown in Figure 7.

The Bootstrap method (Efron, 1979; Efron and Tibshirani, 1994) is a resampling technique to perform statistical inference directly from the data. The bootstrap is typically computed with a randomized algorithm. The practitioner randomly generates B new datasets (i.e. the Bootstrap samples) by drawing randomly from the original dataset consisting of N values (i.e. the first guess).

The first guess of Bootstrap percentile is represented by the POT daily values of L_x and S_{ul} respectively. The number of resampling is chosen B = 1000.

Considering β and σ as the "shape" and "scale" parameters of the first guess, β_j^* and σ_j^* are the "shape" and "scale" parameters of the Bootstrap samples (j = 1 to 1000). The Bootstrap percentile method determines the standardized variable $z_{\beta_j}^* = \frac{\beta}{\beta_j^*}$ and $z_{\sigma_j}^* = \frac{\sigma}{\sigma_j^*}$.

In this way, the appropriate limiting values of the standardized parameters may be directly read from the list of their B estimates ranked in descending order of magnitude (j from 1 to 1000).

Following Meeker et al. (2017), in order to identify the bounding values of β and σ corresponding to the 95% confidence interval, we compute $B^*(\alpha/2)$=1000*(0.05/2)=25 which means that in the ranked values of $z^*_{\beta_j}$ and $z^*_{\sigma_j}$ the 25th value is the upper percentile value, i.e. $z^*_{\beta_{upper}}$ and $z^*_{\sigma_{upper}}$ respectively. Similarly, *B**(1-(*α*/2)) = 1000 (1-(0.05/2)) = 975 means that the 975th value is the lower percentile value $z^*_{\beta_{lower}}$ and $z^*_{\sigma_{lower}}$ respectively.

The upper and lower values di *β* and *σ* corresponding to the 95% confidence interval are then computed from the upper level and lower values of z^*_{β} and z^*_{σ} as it follows:

$$[\beta_{lower}, \beta_{upper}] = \left[z^*_{\beta_{lower}} * \beta, z^*_{\beta_{upper}} * \beta\right] \quad (5)$$

$$[\sigma_{lower}, \sigma_{upper}] = \left[z^*_{\sigma_{lower}} * \sigma, z^*_{\sigma_{upper}} * \sigma\right] \quad (6)$$

Finding these upper and lower values of the Weibull distribution parameters, makes it possible to have the probability curves of the prediction of the extreme values of L_x and S_{ul} shown in Fig. 7a and Fig. 7b along with the 95% confidence intervals.

APPENDIX C

For sea level rise, the average value in the Northern Adriatic Sea is ~3 mm/year (Bonaduce et al., 2016). If we consider the mean sea level tendency equation for semi-enclosed seas (Pinardi et al., 2014) the net volume flux at Otranto that could balance such change is:

$$\frac{\partial}{\partial t}\langle\eta\rangle \sim \frac{T_r}{\Omega}$$

where η is the sea level, the backets indicate the Adriatic Sea area average, T_r is the net volume transport at the Otranto Strait and Ω is the Adriatic Sea surface area. If we take the 3 mm/year for the left hand side of the equation, the value of deduced transport is 133 m3/sec. If we compare now this change with the observed values of

Otranto Strait Transport that are of the order of 10^5 m3/sec the change in transport due to sea level rise is 0.1%.

CODE AVAILABILITY

The CMCC EBM is free and open software under the terms of the LGPL license, distributed from its web page (http://www.estuaryboxmodel.org) where a Test Case on Po di Goro estuary with the model inputs and outputs are accessible and interoperable.

DATA AVAILABILITY

The data archiving of CMCC EBM historical simulations and future projections here discussed is underway on the webpage; in the meantime, the EBM input data and results are included as supplementary material.

The observational datasets used in this study for the calibration and validation of the CMCC EBM are publicly available. The observations of salinity at the Po di Goro mouth (Manufatto gauge) and the Po river runoff at the Pontelagoscuro station are findable through the Arpae repository and accessible at the Arpae webapp (https://simc.arpae.it/dext3r).

AUTHOR CONTRIBUTION

Conceptualization: GV, NP

Methodology: SMK, GV, NP, GC

Investigation: SMK, GV

Visualization: SMK, GV

Writing—original draft: SMK, GV

Writing—review & editing: SMK, GV, NP, GC

ACKNOWLEDGEMENTS

The authors are grateful to the Regional Agency for Prevention, Environment and Energy of Emilia-Romagna (Arpae) for providing the salinity observations at the Manufatto gauge and the Po river runoff data at the Pontelagoscuro station. The authors thank Dr. Silvio Gualdi and the CSP Division of CMCC Foundation for sharing the 3D ocean forcing used in this study.

This research was funded by the OPERANDUM project and the EU Copernicus Marine Environment Monitoring Service projects of the Mediterranean Sea Monitoring and Forecasting (n. 74-351 CMEMS-MFC-MED-N). OPERANDUM project has received funding from the European Union’s Horizon 2020 research and innovation program under grant agreement No. 776848.

.

BIBLIOGRAPHY

Adloff, F., Jordà, G., Somot, S., Sevault, F., Arsouze, T., Meyssignac, B., ... & Planton, S.: Improving sea level simulation in Mediterranean regional climate models. Climate dynamics, 51(3), 1167-1178, doi:10.1007/s00382-017-3842-3, 2018.

Barenblatt, G.I.: Dimensional analysis, CRC Press, ISBN: 88124226X, 9782881242267, 1987.

Bellafiore, D., Ferrarin, C., Maicu, F., Manfe, G., Lorenzetti, G., Umgiesser, G., Zaggia, L., and Levinson, A.V.: Saltwater intrusion in a Mediterranean delta under a changing climate, J. Geo. Res.: Oceans. 126(2), doi:10.1029/2020JC016437, 2021.

Bucchignani, E., Montesarchio, M., Zollo, A., and Mercogliano, P.: Regional climate simulations with COSMO-CLM over the Mediterranean area, Adv. Climate Sci. 338-351, 2014.

Bonaduce, A., Pinardi, N., Oddo, P. *et al.* 2016. Sea-level variability in the Mediterranean Sea from altimetry and tide gauges. *Clim Dyn* **47,** 2851–2866, 10.1007/s00382-016-3001-2.

Cavicchia, L., Gualdi, S., Sanna, A., and Oddo, P.: The regional ocean-atmosphere coupled model COSMO-NEMO MFS. CMCC Research Paper. Issue RP0254, 2015.

Claussen, M., Mysak, L., and Weaver, A.: Earth system models of intermediate complexity: closing the gap in the spectrum of climate system models, Climate Dynamics. 18, 579-586, doi:10.1007/s00382-001-0200-1, 2002.

Efron, B.: Bootstrap Method: Another Look at the Jackknife, The annals of Statistics. 9, 1-26, url: https://www.jstor.org/stable/2958830, 1979.

Efron, B., and Tibshirani, R.J.: An Introduction to the Bootstrap, Chapman and Hall, 1-436, 1994.

Egbert, D., and Erofeeva, S.Y.: Efficient inverse modeling of barotropic ocean tides, J. Atm. Oceanic Tech. 19(2), 183-204, doi:10.1175/1520-0426(2002)019<0183:EIMOBO>2.0.CO;2, 2002.

Green, T.R.: Linking Climate Change and Groundwater in Integrated Groundwater Management: Concepts, Approaches and Challenges, Spr. Int. Pub., 97-141, doi:10.1007/978-3-319-23576-9_5, 2016.

James, N.C., van Niekerk, L., Whitfield, A.K., Potts, W.M., Götz, A., and Paterson, A.W.: Effects of climate change on South African estuaries and associated fish species, Climate Res. 57, 233-248, 2013.

Guangpeng, L., Bracco A. and S. Daoxun, 2022. Offshore Freshwater Pathways in the Northern Gulf of Mexico: Impacts of Modeling Choices, Frontiers in Marine Science, 9, 10.3389/fmars.2022.841900.

Kurdistani, S. M., Tomasicchio, G. R., D'Alessandro, F., and Hassanabadi, L.: River bank protection from ship-induced waves and river flow, Water Sci. Eng., 12(2), 129–135, doi:10.1016/j.wse.2019.05.002, 2019.

Leadbetter, M.R.: On a basis for 'Peaks over Threshold' modeling, Statistics and Probability Letters, 12, 357-362, doi: 10.1016/0167-7152(91)90107-3, 1991.

MacCready, P., and Geyer, W. R.: Advances in Estuarine Physics, Annu. Rev. Marine. Sci. 2(1), 35-58, doi:10.1146/annurev-marine-120308-081015, 2010.

Meeker, W.Q., Hahn, G.J., and Escobar, L.A.: Statistical Intervals, JOHN WILEY and SONS, 1-578, ISBN-10: 0471687170, 2017.

Pinardi, N., Bonaduce, A., Navarra, A., Dobricic, S., & Oddo, P.: The mean sea level equation and its application to the Mediterranean Sea. *Journal of climate*, *27*(1), 442-447, 2014.

Sardeshmukh, P.D., and Compo, G.P.: Need for Caution in Interpreting Extreme Weather Statistics, J. Climate. 28, 9166-9187, doi:10.1175/JCLI-D-15-0020.1, 2015.

Scoccimarro, E., Gualdi, S., Bellucci, A., Sanna, A., Fogli, P.G., Manzini, E., Vichi, M., Oddo, P., and Navarra, A.: Effects of Tropical Cyclones on Ocean Heat Transport in a High-Resolution Coupled General Circulation Model, J. Climate. 24(6), 4368-4384, doi:10.1175/2011JCLI4104.1, 2011.

Sepp Neves, A.A., inardi, N., Navarra, A., and Trotta, F.: A General Methodology for Beached Oil Spill Hazard Mapping, Front. Mar. Sci. 7, 1-10, doi:10.3389/fmars.2020.00065, 2020.

Somot, S., Ruti, P., Ahrens, B., Coppola, E., Jordà, G., Sannino, G., & Solmon, F.: Editorial for the Med-CORDEX special issue, Climate Dynamics, 51(3), 771-777, doi:10.1007/s00382-018-4325-x, 2018.

Sun, Q., Whitney, M.M., Bryan, F.O., and Tseng, Y.H.: A box model for representing estuarine physical processes in Earth system models, Ocean Modelling, 112, 139-153, doi:10.1016/j.ocemod.2017.03.004, 2017.

Torresan, S., Gallina, V., Gualdi, S., Bellafiore, D., Umgiesser, G., Carniel, S., ... Critto, A.: Assessment of climate change impacts in the North Adriatic coastal area, Part I: a multi-model chain for the definition of climate change hazard scenarios, Water, 11(6), 1157, doi: 10.3390/w11061157, 2019.

Verri, G., Pinardi, N., Bryan, F., Tseng, Y., Coppini, G., and Clementi, E.: A box model to represent estuarine dynamics in mesoscale resolution ocean models, Ocean Modeling. 148, 1-14, doi:10.1016/j.ocemod.2020.101587, 2020.

Verri, G., Kurdistani, S.M., Coppini, G., and Valentini, A.: Recent advances of a box model to represent the estuarine dynamics: time-variable estuary length and eddy diffusivity, J. Adv. Mod. Earth Sys. (JAMES). 13(4), 1-16, doi: 10.1029/2020MS002276, 2021.

Verri, G., Pinardi, N., Oddo, P., Ciliberti, S.A., and Coppini, G.: River runoff influences on the Central Mediterranean Overturning Circulation, Climate Dynamics. 50(5-6), 1675–1703, doi:10.1007/s00382-017-3715-9, 2018.

Vezzoli, R., Mercogliano, P., Pecora, S., Zollo, A., and Cacciamani, C.: Hydrological simulation of Po River (North Italy) discharge under climate change scenarios using the RCM COSMO-CLM. Sci. Total Env. 521(2), 346-358, doi:10.1016/j.scitotenv.2015.03.096, 2015.

Watanabe, K., Kasai, A., Antonio, E.S., Suzuki, K., Ueno, M., and Yamashita, Y.: Influence of salt-wedge intrusion on ecological processes at lower trophic levels in the Yura Estuary, Japan, Est. Coastal Shelf Sci. 139, 67-77, doi:10.1016/j.ecss.2013.12.018, 2014.

Weibull, W.: A Statistical Distribution Function of Wide Applicability, ASME J. App. Mech. – Trans. American Soc. Mech. Eng., 293-297, 1951.

Yari, S., Kovacevic, V., Cardin, V., Gacic, M. and H.Briden, 2012. Direct estimate of water, heat, and salt transport through the Strait of Otranto. J. Geophys. Res., 117, C9, 10.1029/2012JC007936

Yeung Leung, A. Tsz , Stronach, J., and Matthieu, J.: Modelling Behaviour of the Salt Wedge in the Fraser River and Its Relationship with Climate and Man-Made Changes, J. of Mar. Sci. and Eng., 6(4), 130: 1-29, doi:10.3390/jmse6040130, 2018.

Figure 1. The Goro branch of the Po river; it has a river-dominated estuary and flows into the micro-tidal Adriatic Sea

Imagery ©2021 Google, Landsat / Copernicus, Data SIO, NOAA, U.S. Navy, NGA, GEBCO, Imagery ©2021 TerraMetrics, Map data ©2021 5 km

Figure 2. Pontelagoscuro hydrometry station. (a) observed discharge values during (1982 – 2011), (b) predicted discharge values for the scenario period (2021–2050)

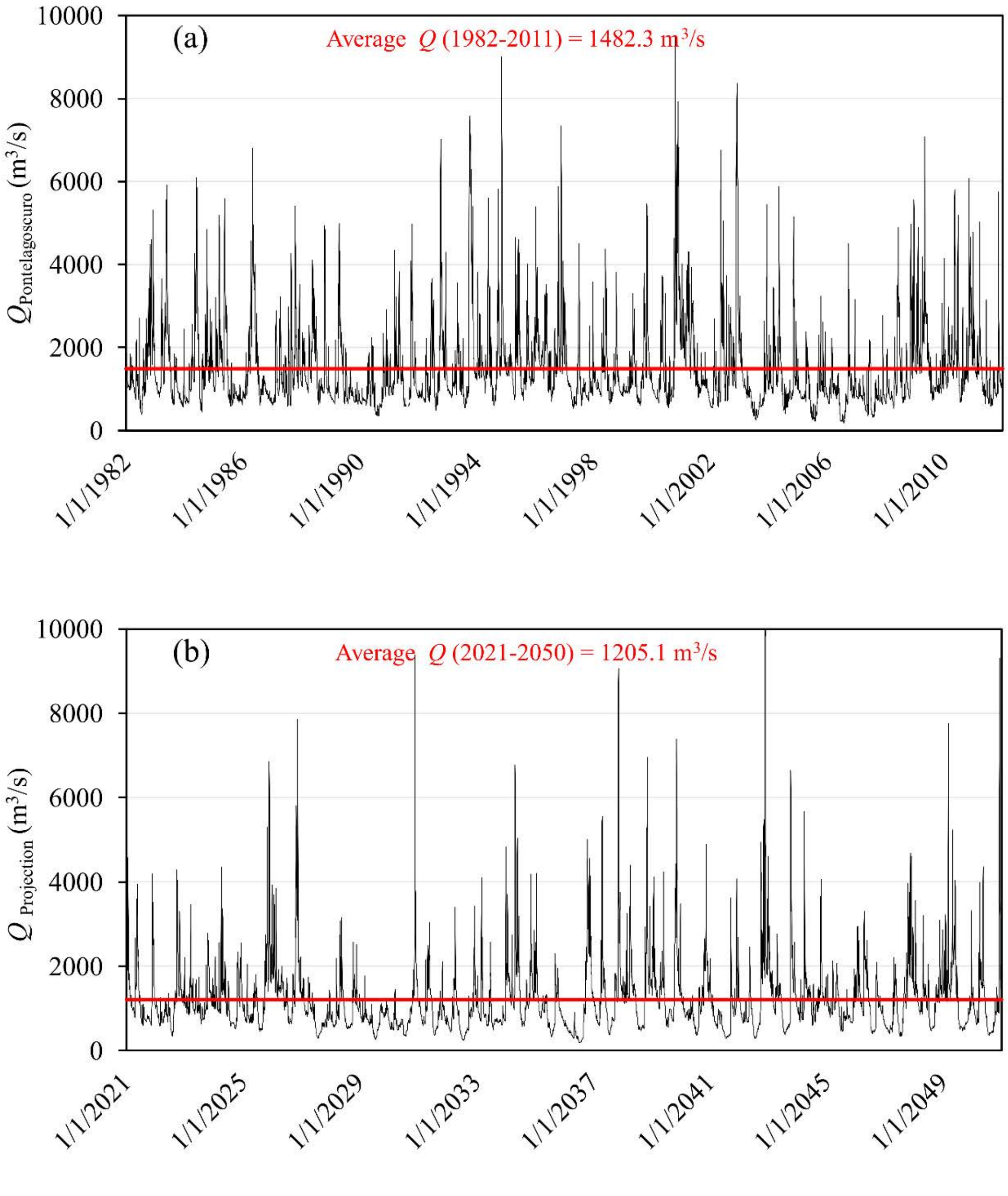

Figure 3. Salt-wedge intrusion (EBM model). (a) historical period (1982-2011), (b) scenario period (2021–2050)

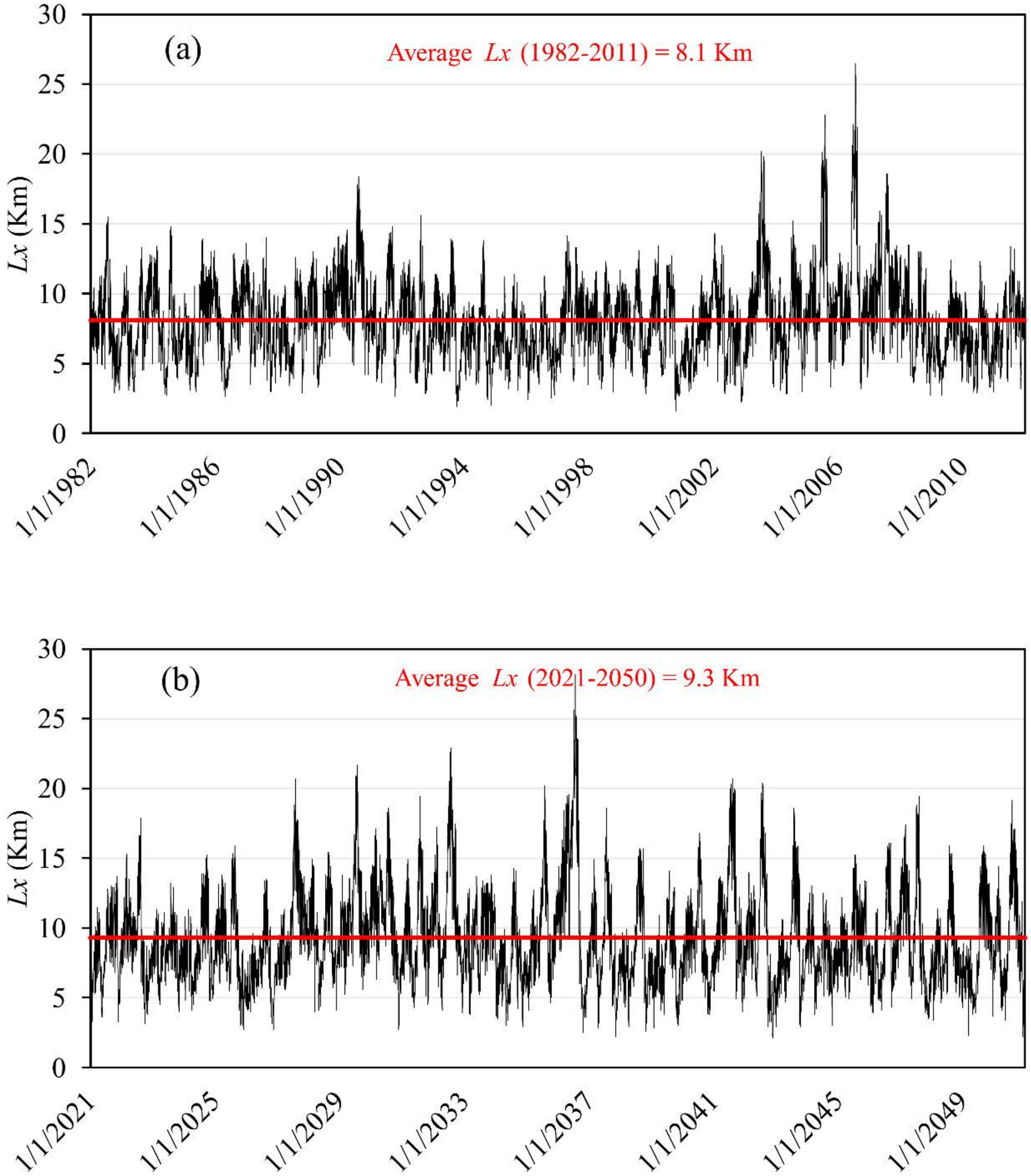

Figure 4. Outflowing salinity (EBM model). (a) historical period (1982-2011), (b) scenario period (2021–2050)

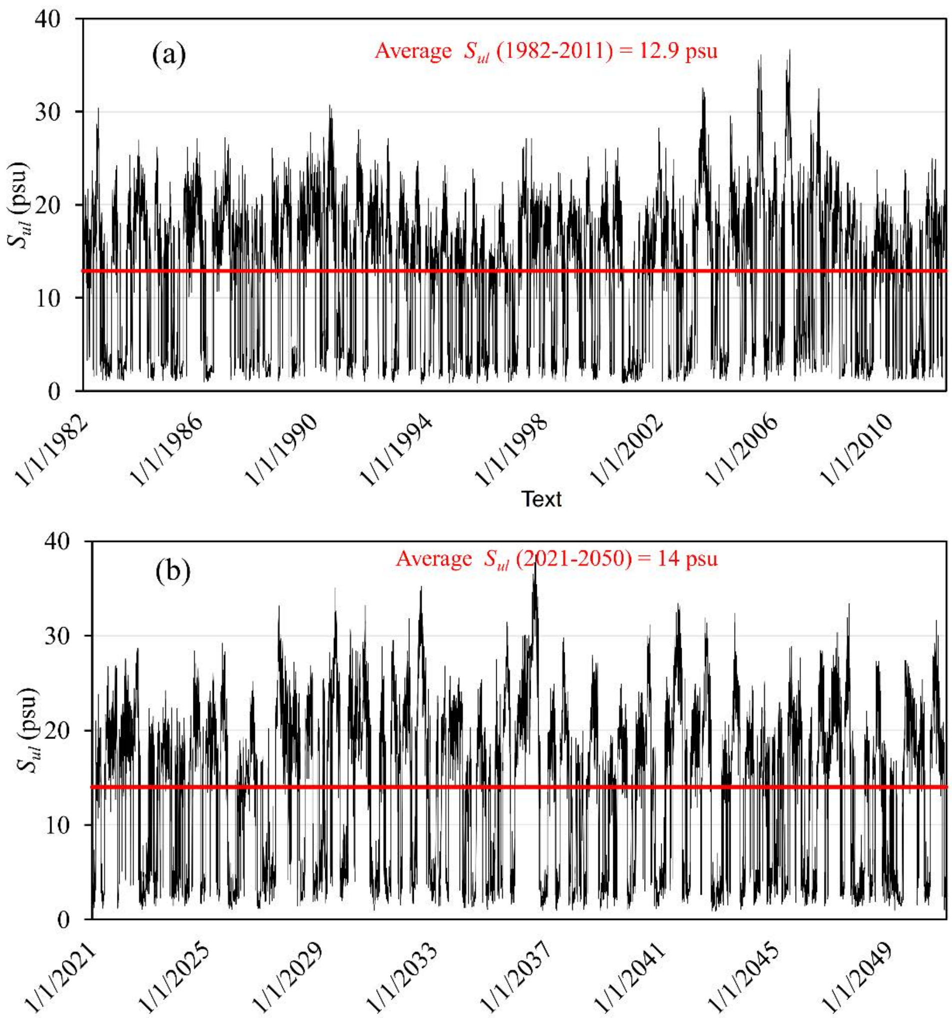

Figure 5. Seasonal cycle of daily mean values (EBM model). (a) Salt-wedge intrusion, (b) Outflowing salinity

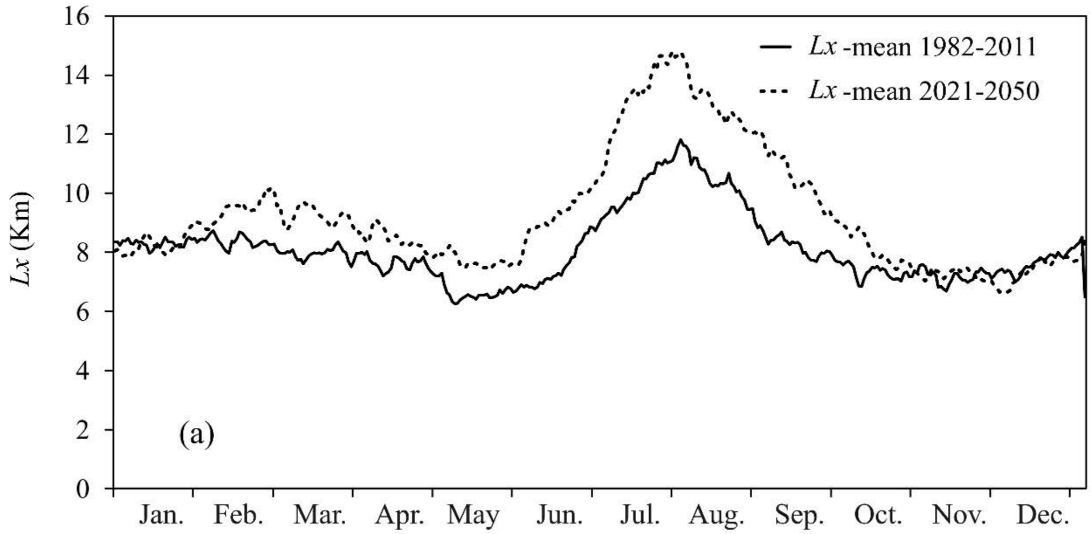

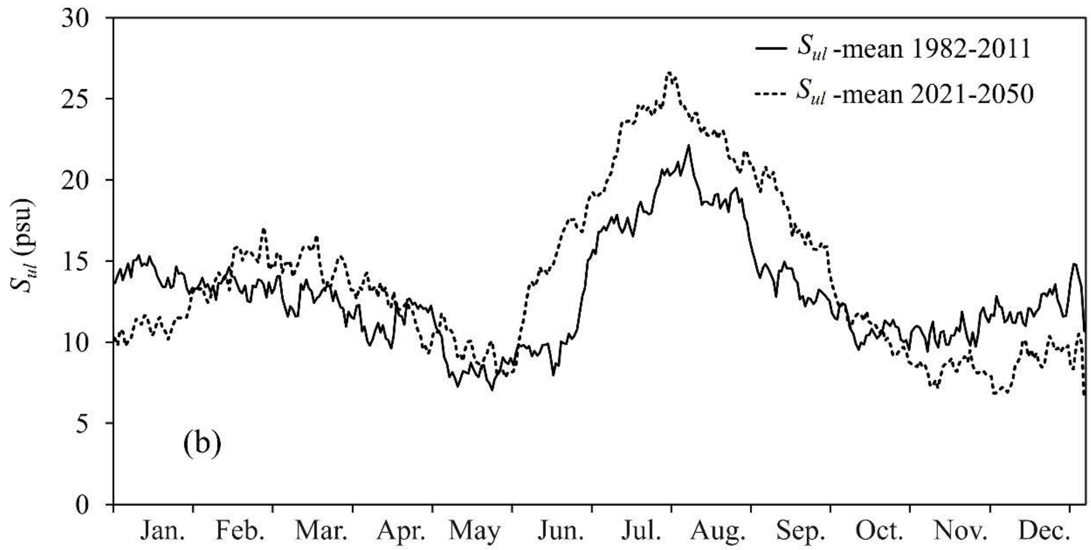

Figure 6. Frequencies of occurrence of daily values. (a) Salt-wedge intrusion, (b) Outflowing salinity

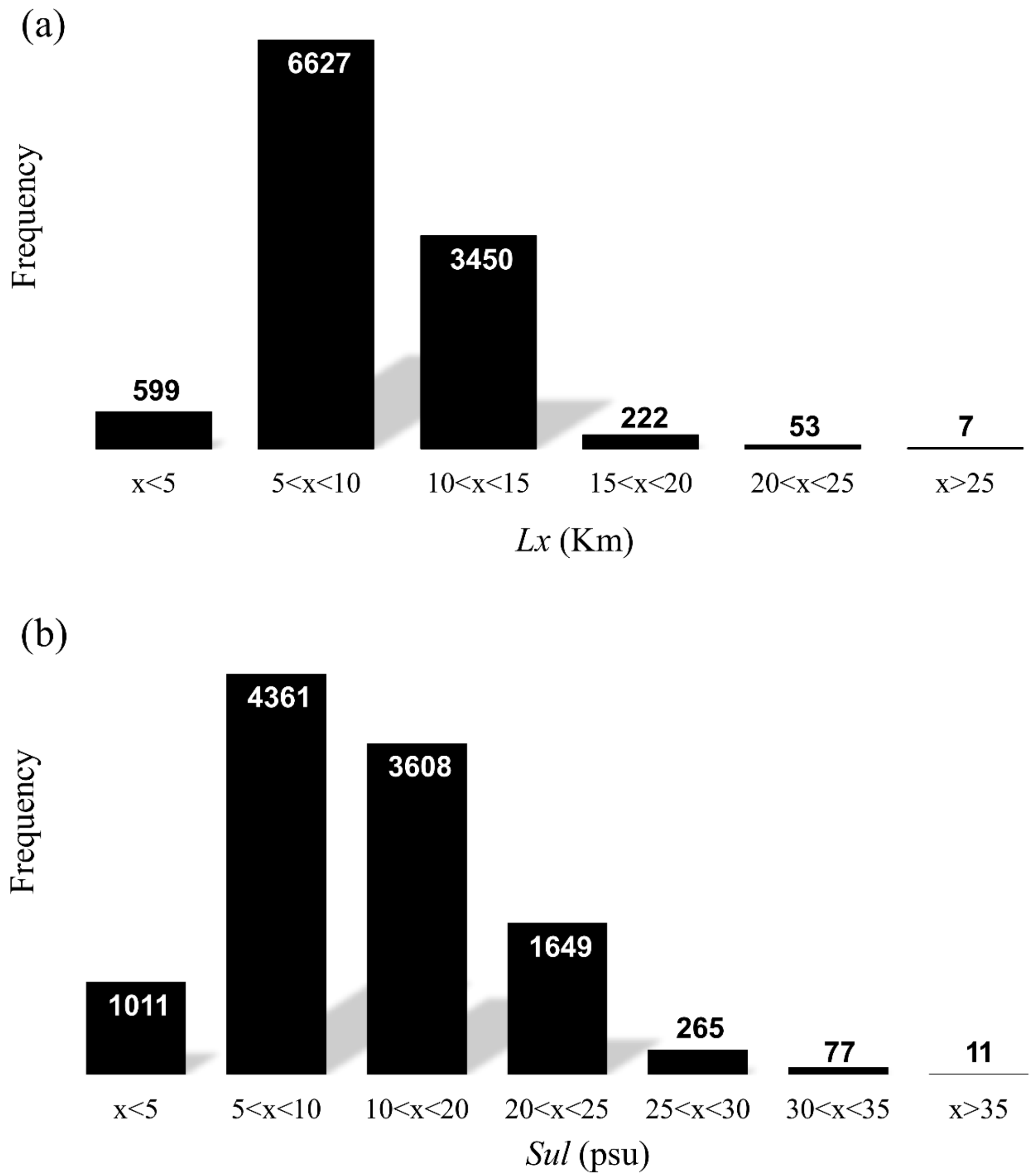

Figure 7. Probability curves with upper-lower 95% confidence intervals. (A) Compared with the predicted values of Lx for the scenario period (2021-2050), (B) Compared with the predicted values of the outflowing salinity for the scenario period (2021-2050)

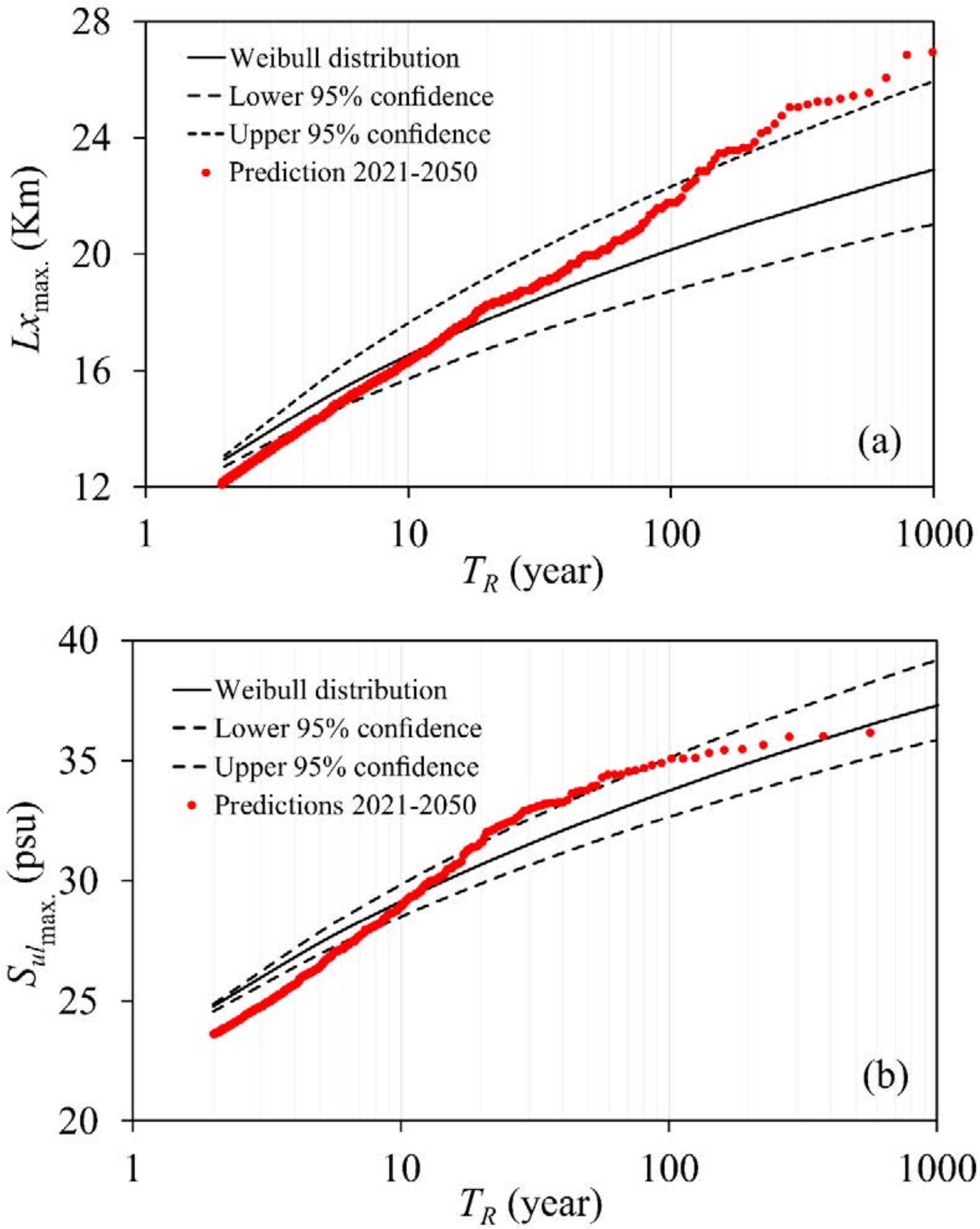

Figure A.1 Sketch of the EBM model. Black arrows stand for input variables coming from coupled models or observational datasets, red arrows indicate the unknowns solved by the EBM. The pairs of blue arrows represent the tidal mixing. The model source code is open and free and it is available here: http://www.estuaryboxmodel.com